SSRG International Journal of Electronics and Communication Engineering
ISSN: 2348-8549/ https://doi.org/10.14445/23488549/IJECE-V12I11P105

Volume 12 Issue 11, 43-56, November 2025

Original Article

An Efficient IoT-Driven Health Care Monitoring System using Advanced Metaheuristic Optimisation Algorithms with Spiking Neural Network for Smart Diagnosis

Fatimah Alqahtani[1], Betty Elezebeth Samuel[2], Rasitha Banu GulMohamed[3], Vidya Sivalingam[4], Anjali Gupta[5], Nithinsha Shajahan[6]

[1,2,4,5,6]*Department of Computer Science, College of Engineering and Computer Sciences, Jazan University, Jazan, SaudiArabia.*
[3]*Health Informatics Program, Department of Public Health, College of Nursing and Health Sciences, Jazan University, Jazan, Saudi Arabia.*

[4]*Corresponding Author : vsivalingam@jazanu.edu.sa*

Received: 05 September 2025 Revised: 07 October 2025 Accepted: 06 November 2025 Published: 29 November 2025

Abstract - *Since the population is rising worldwide, a vast need arises to deliver appropriate medical care services. The sensor is an effective technology primarily employed to enable the Internet of Things (IoT)- based healthcare monitoring method. The IoT is transporting a novel revolution in research and academia. It has powerful roots, which are producing amazing variations in numerous areas, especially healthcare. IoT healthcare methods enable patients to receive personalized care by remotely monitoring their conditions. IoT applications are primarily beneficial for delivering healthcare, as they allow secure and real-time remote patient monitoring. In recent times, the traditional linear method has been replaced by innovative techniques of Artificial Intelligence (AI) and Machine Learning (ML). Whereas, Deep Learning (DL) is a sub-field of ML, which is much more trustworthy and stronger to certainly manage and study from a vast quantity of intricate healthcare data, and provides actionable visions and solutions to complex issues. This study proposes an Efficient Health Care Monitoring System using Advanced Metaheuristic Optimisation Algorithms and Spiking Neural Network Method for Smart Diagnosis (EHCMS-MOASNN) model for Smart Diagnosis in IoT. The primary objective of the EHCMS-MOASNN technique is to develop a smart healthcare monitoring system for the medical sector utilizing advanced models. Initially, the data pre-processing applies the min-max scaling method to convert input data into an appropriate format. Furthermore, the feature selection process is implemented using the Binary Grouper and Moray Eel (BGME) optimization approach to detect and select the most relevant and significant features in the input data. For the classification process, the EHCMS-MOASNN technique implements the Spiking Neural Network (SNN) approach. Additionally, the Mountain Gazelle Optimiser (MGO)-based hyperparameter tuning is performed. The comparison analysis of the EHCMS-MOASNN method demonstrated a superior accuracy value of 99.12% over recent techniques under the Healthcare IoT dataset.*

Keywords *- Health Care Monitoring, IoT, Metaheuristic Optimisation Algorithms, Spiking Neural Network, Smart Diagnosis.*

1. Introduction

The IoT enables the connection of physical objects to the Internet, allowing data to be sent or received over the Network [1]. The IoT concepts are advanced from diverse techniques such as machine learning, real-time analysis, embedded systems, and sensors. This is all about the smart hospital devices and concepts influenced by Wireless or fixed Internet. Smart devices can collect information and share it in everyday life to accomplish the necessary tasks [2]. IoT applications reach cars, devices, entertainment systems, smart cities, connected healthcare, and homes. Numerous medical devices, sensors, diagnostics, AI, and advanced imaging technologies are vital to the implementation of IoT in the medical field [3]. This device improves the efficiency and standard of living in both new and old societies and industries. IoT associates all mechanical, digital technologies, and computing for transferring information over the Internet without human interaction. Currently, IoT has emerged as a key area of development, enabling the progression of healthcare monitoring systems [4]. The IoT healthcare monitoring system allows precise tracking of individuals. It connects various devices and services worldwide over the Internet to collect, share, monitor, store, and analyze the data generated by these devices [5]. Analyzing illnesses and observing patients is vital to providing adequate medical care, and

employing sensor networks in the human body can significantly support these endeavours. Moreover, the data is readily available anywhere and at any time worldwide. Figure 1 portrays the general framework of the IoT healthcare monitoring system.

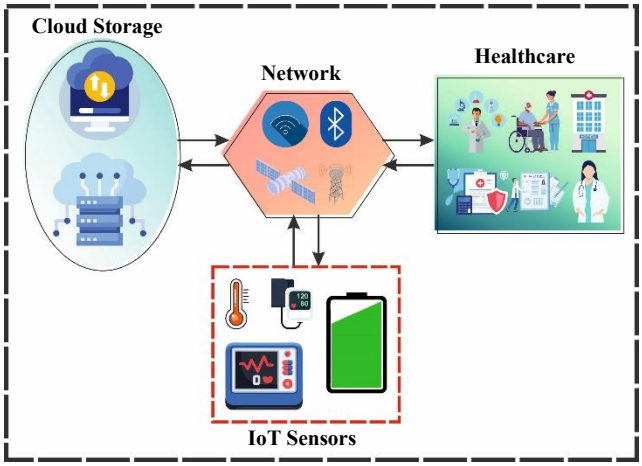

Fig. 1 General structure of an IoT-based healthcare system

Patients with serious injuries or from specific regions might have trouble reaching the hospital. Hence, patients will utilize video conferencing to connect with their doctors, improving their health while saving time and money. They may use these technologies to record their health conditions on their mobile devices [6]. It is expected that the advantages of the IoT will be developed, resulting in customized treatment that improves patient outcomes by reducing healthcare management costs. IoT methods enable doctors to monitor their patients and schedule appointments remotely and efficiently. Patients can also enhance their home healthcare by reducing the need to visit doctors and the risk of receiving inappropriate or unnecessary medical treatment in clinics or hospitals [7]. Therefore, the quality of medical care and the general safety of patients will improve, while the overall care expenses may decrease.

The IoT plays a crucial role in healthcare. Soon, we will have access to a home-based health monitoring system that enhances convenience and streamlines the hospital process [8]. IoT sensors must be closely organized to monitor the environment and the body constantly. Ahead of computer-generated consultations for remote medical care, the IoT can provide an effective data connection to multiple locations [9]. Predictive analytics in healthcare encompasses various methods, ranging from conventional linear techniques to advanced algorithms of ML and AI. DL, a subfield of ML, is sufficiently dependable and robust to learn and adapt from a vast volume of complex healthcare data, providing insights and solutions to challenging problems. It is deployed to a broad range of medical applications and has exceeded the outcomes of classical methods [10]. Connected technologies are creating new possibilities to enhance patient monitoring and diagnosis. By incorporating advanced approaches with bio-inspired neural models, healthcare systems can facilitate faster and more accurate decision-making. This improves early detection, reduces manual effort, and enables real-time, personalized care.

This study proposes an Efficient Health Care Monitoring System using Advanced Metaheuristic Optimisation Algorithms and Spiking Neural Network Method for Smart Diagnosis (EHCMS-MOASNN) model for Smart Diagnosis in IoT. The primary objective of the EHCMS-MOASNN technique is to develop a smart healthcare monitoring system for the medical sector utilizing advanced models. Initially, the data pre-processing applies the min-max scaling method to convert input data into an appropriate format. Furthermore, the feature selection process is implemented using the Binary Grouper and Moray Eel (BGME) optimization approach to detect and select the most relevant and significant features in the input data. For the classification process, the EHCMS-MOASNN technique implements the Spiking Neural Network (SNN) approach. Additionally, the Mountain Gazelle Optimiser (MGO)-based hyperparameter tuning is performed to optimize the classification outcomes of the SNN approach. The efficiency of the EHCMS-MOASNN method is validated by comprehensive studies using the Healthcare IoT dataset.

The significant contribution is listed below.

- The min-max normalization is used for scaling diverse IoT sensor data into a consistent range, enabling smoother model training. The data uniformity that stabilizes the learning and mitigates the impact of outliers is improved. The process effectually contributes to improving efficiency and accuracy in real-time health monitoring applications by enhancing convergence speed and classification results.
- The novel BGME-based hybrid feature selection method is employed to identify the most relevant and non-redundant features from high-dimensional intrinsic health data. The computational overhead is reduced while preserving crucial diagnostic data. This also enhances the interpretability, processing speed, and overall diagnostic performance of the model.
- The classification utilizes SNN for handling temporal and event-driven IoT health data. This model is enabling precise pattern recognition with lesser energy consumption compared to conventional DL techniques. Their event-based processing is well-suited for real-time health monitoring scenarios. This integration enhances diagnostic accuracy while ensuring energy-efficient performance in IoT environments.
- The MGO technique is used for tuning the SNN hyperparameters and is motivated by the strategic foraging behaviour of gazelles. This optimization improves convergence speed and also ensures optimal parameter selection for superior performance. MGO effectively navigates the complex search space to avoid

local optima. Its integration enhances classification accuracy and overall system robustness.

- A novel hybrid framework is proposed by integrating BGME-based feature selection with an MGO-tuned SNN classifier. This architecture enables precise, rapid, and resource-efficient processing of real-time health sensor data. Its novelty is in the synergistic optimization of feature relevance and neural efficiency for superior diagnostic outcomes.

2. Literature Survey

Vasanth et al. [11] focused on the integration of IoT and ML, examining their applications in the healthcare sector. They can advance progress in diagnosis, clinical outcomes, and alter patient treatments. By integrating ML models with IoT devices, healthcare specialists can obtain and analyze massive volumes of data. Sudha et al. [12] proposed a novel technique for stress management-centred predictive models of healthcare workers' wellness using machine learning and cloud computing. Utilizing numerous information sources, the models compile data from social media, EHR, surveys, and wearable devices within a single position to investigate. Predicting methods forecast healthcare workers' wellness and stress levels, which was advanced by employing adaptive boosting, an ML method. In [13], IoT-assisted remote patient monitoring systems provide real-time insights into patients' health parameters, enabling patient participation and informed decision-making. The key hub of these methods presents precise and up-to-date patient information, enabling prompt messaging regarding chronic diseases. EHR presents extensive historical health information while safeguarding security and privacy. However, difficulties such as scalability, interoperability, and data security remain. Najim et al. [14] introduced an IoT and WSN structure for monitoring patients in higher-speed 5G communications. According to the Artificial Neural Network (ANN), intelligent health monitoring systems have been advanced by utilizing IoT tools. Additionally, this method helps senior citizens, especially in serious situations at home, communicate and update their medical conditions to the hospital, which will be addressed promptly, particularly in remote regions.

Rajarajan et al. [15] presented a real-time Recurrent Neural Network (RNN) respiratory pattern monitoring system that will be combined with IoT. Respiratory rate, Tidal volume, and expiratory and inspiratory flow models are some of the respiratory features that are monitored remotely utilizing our method of IoT sensors, which gather information continuously. An RNN method analyzes patterns in the chart of respiratory signals and provides an immediate response to the patient's condition based on data processing. In [16], a BC-orchestrated DL methodology for Secure Data Transmission in IoT-aided healthcare systems, otherwise known as the "BDSDT" model. BDSDT also utilizes the off-chain storage InterPlanetary File System (IPFS) model, and an Ethereum smart contract is employed to address data security concerns. Parameshachari et al. [17] examined unique methods for the automated creation of CNN topology and also established a novel technique for analysis. It proposes an IoT-based healthcare system that enables real-time monitoring of environmental factors and active signals for different patients. It encompasses five sensors, which were used to gather information from the hospital location. Khanna et al. [18] proposed an original IoT and DL-based Healthcare Disease Diagnosis (IoTDL-HDD) method employing a biomedical ECG signal. Moreover, the introduced IoTDL-HDD method employs a BiLSTM feature removal procedure to remove beneficial feature directions from the ECG signal. To improve the efficacy of the BiLSTM model, the Artificial Flora Optimization (AFO) model was used as a hyperparameter optimization. Thrimurthulu et al. [19] proposed the Context-Aware Architecture IoT Healthcare Monitoring System (CAA-IoT-HMS) with Periodic Implicit Generative Adversarial Networks (PIGAN) technique, utilizing the Harbour Seal Whiskers Optimisation Algorithm (HSWOA) method to improve classification accuracy and overall system performance.

Basavaiah et al. [20] introduced an IoT-based epilepsy monitoring system by utilizing sensors and ML models for accurate seizure detection and prediction. The Convolutional Neural Network (CNN), Random Forest (RF), and Logistic Regression (LR) models are incorporated to enable continuous remote monitoring and timely alerts for effective intervention. Mangal and Lakshmi [21] explored biomedical signal processing techniques to enhance the acquisition and pre-processing of physiological signals, thereby improving data quality in real-time health monitoring systems. Arivalahan and Vinoth [22] introduced the DCSNN-WMA-Healthcare Monitoring IoT-Context Aware Architecture (DCSNN-WMA-HCM-IoT-CAA) method to improve classification accuracy, reduce computation time, and enhance overall system performance. Ghosh et al. [23] developed BlockFaaS, a blockchain-assisted serverless framework incorporating advanced AI models for secure, energy-efficient, and real-time healthcare applications. The AIBLOCK is integrated with dynamic sharding and zero-knowledge proofs, utilizing HealthFaaS for enhanced cardiovascular risk detection while ensuring data privacy and interpretability through explainable AI and Federated Learning (FL). Suryawanshi et al. [24] presented the Cell Attention Spiking Neural Network (CASNN) model. The Hybrid Mud Ring Osprey Optimisation Algorithm (HMROOA) is employed for feature selection, while the War Strategy Optimisation (WSO) method is used for tuning. Alshuhail et al. [25] presented an IoT-based health monitoring system utilizing adaptive mesh networking and hybrid sensor fusion algorithms. The model enables real-time edge AI analytics and secure, scalable data sharing. Gautam and Sharma [26] introduced a technique by integrating Artificial Narrow Intelligence (ANI) with neuromorphic computing. The model utilizes neuromorphic hardware to

improve speed, accuracy, and adaptability in patient monitoring and diagnostic systems.

Existing studies highlight limitations, including challenges in scalability, interoperability, and ensuring robust data security and privacy. Several techniques rely heavily on specific sensor types or limited data sources, which can affect their generalizability across diverse healthcare environments. Moreover, real-time processing and accurate prediction remain constrained by computational complexity and suboptimal feature selection methods. Although models such as DL and ANN are energy-efficient and adaptable across heterogeneous IoT data, they still require enhancement. Furthermore, integration of advanced optimization algorithms for tuning model parameters is not adequately addressed. The limitations also include challenges with scalability, real-time processing efficiency, and comprehensive integration of privacy-preserving mechanisms. The research gap lies in developing a comprehensive framework that addresses these limitations by enabling efficient, secure, and accurate health monitoring with optimized feature selection and classification tailored to IoT ecosystems.

3. The Proposed Framework

In this study, we have proposed an EHCMS-MOASNN methodology for Smart Diagnosis in IoT. The primary objective of the EHCMS-MOASNN technique is to develop a smart healthcare monitoring system for the medical sector utilizing advanced models. It contains four distinct stages: min-max scaling, binary optimization process, classification process, and parameter fine-tuning. Figure 2 represents the flow of the EHCMS-MOASNN technique.

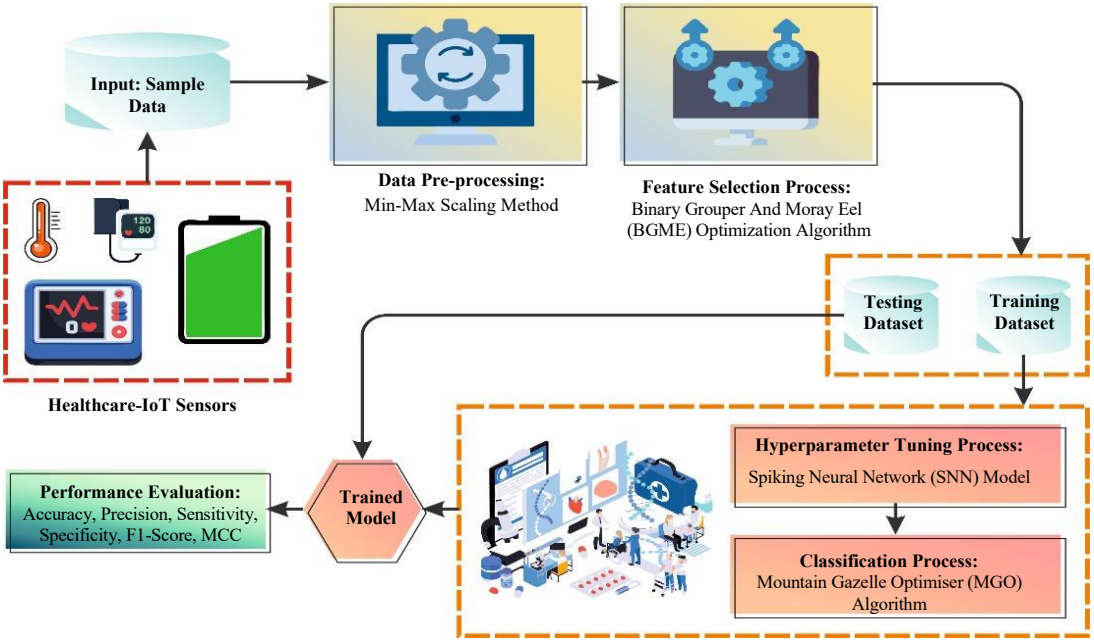

Fig. 2 Workflow of EHCMS-MOASNN model

3.1. Stage I: Min-Max Scaling

Initially, the data pre-processing applies the min-max scaling method to convert the input data into an appropriate format. To normalize the input features between 0 and 1, it employs a Min-Max scaling that enhances the execution of the following methodologies [27]. Given a feature x_i, the transformation is:

$$x_i' = \frac{x_i - min(x)}{max(x) - min(x)} \quad (1)$$

Here, x_i represents the original value. $\max(x)$ and $\min(x)$ represent the maximum and minimum values of the feature across each sample. The effective training of DL techniques is reliant on normalization, which ensures coherence through several sizes of features.

3.2. Stage II: Feature Selection using BGME Model

Additionally, the FS process is implemented using the BGME optimization algorithm to detect and select the most relevant and significant features in the input data. GME is a novel technique stimulated by the association between moray eels and groupers, each of which employs a distinct attack tactic [28]. When these dual predators unite their hunting abilities, the prey has a low probability of survival because many agents are hunting for prey with divergent tactics and rapid access to resources. This cooperative conduct proposes a higher level of intellect. The foraging among similar species produces inferior results in comparison to the collaboration among the moray eels and groupers. In the foraging procedure, the grouper and Moray eel cooperate in 4 states: Primary Search (PS), Encircling Search (ES), Pair Association (PA), and Attacking and Catching (AC). It is highly essential to

develop a BGME, which is applied to the selection of a feature problem. A 1D vector signifies every solution, and its span is dependent upon the number of features. The 1 or 0 values are assigned to each element in the vector. The value of 1 depicts that the corresponding feature is chosen, whereas zero shows that the feature is not selected. Therefore, to execute the GME for the feature selection issue, a mapping device from real value to binary space must be executed by employing the sigmoid function, utilizing Equations (2) and (3).

$$Sigmoid\ (Y_m^i) = \frac{1}{1 + e^{-Y_m^i}} \tag{2}$$

$$Y_{binary\_m}^i(i+1) = \begin{cases} 1 & if\ rand(0,1) \geq sigmoid(Y_m^i) \\ 0 & otherwise \end{cases} \tag{3}$$

BGME begins with search agents (S) that form a group, which is denoted as Y. Let P represent the total number of iterations. And the number of iterations (P_{As}) equals 1. Thus, the number of iterations for PS, ES, and AC is signified as $P_{\_Search}$, $PEnc$, and PAC, which are formulated in Equations (4) – (6)

$$P_{Search} = \left\lfloor \frac{P}{3} \right\rfloor \tag{4}$$

$$P_{Enc} = \left\lfloor \frac{P}{3} \right\rfloor \tag{5}$$

$$P_{AC} = \left\lfloor P - 2 * \frac{P}{3} \right\rfloor \tag{6}$$

In the PS stage, the grouper starts to travel in a zigzag drive. Next, the m^{th} grouper's upgraded location is concluded by Equation (8), which diverges by the no. of hops. When the no. of hops is even, the novel location is chosen randomly to surpass the present location. When the no. of hops is odd, the novel location is selected at random to be less than the current one while following the east boundary of the hunt region.

$$\text{The Updated Position of } m^{th} \text{ grouper}$$
$$\begin{cases} Y_m^{hop+1} = Rand(Y)\ Where\ Y_m^{hop} < Y \leq max\ (Y_m)\ \ if No.of lzop is\ even \\ Y_m^{hop+1} = Rand(Y)\ Where\ min\ (Y_m) \leq Y < Y_m^{hop}\ if No.of\ hop\ is\ odd \end{cases} \tag{7}$$

In the PA stage, the collaboration between the eels and groupers enables them to discover novel regions of the search area. Every grouper fish correlates with an eel according to the objective function value.

In the ES stage, every pair of actions encloses the prey by travelling independently, thus enabling the search of numerous areas within the searching space. The logarithmic spiral was chosen as the main mechanism for position upgrades for groupers in the ES stage, whereas the sinusoidal wave is employed for upgrading the eel's locations. The prey location is defined as follows. At first, Equation (8) is utilized for computing the differences among the position coordinates ($\Delta y_{\_m}$) of the grouper's location (Y_{gm}) and the location of an eel ($Y_{\_Em}$) for determining the location of prey. The location of prey is formulated in Equation (10).

$$\Delta y_{mj} = \left(Y_{Em} - Y_{gm}\right) \tag{8}$$

$$= \sqrt{\sum_{j=1}^{D} (\Delta y_m)^2} \tag{9}$$

$$c_m = Y_{gm} + \frac{L}{dis} * \Delta y_{mj} \tag{10}$$

Next, the grouper and the eel introduce their respective actions near the prey. The following steps outline the process for upgrading the location of the grouper at this stage. First, define the distance between the grouper and the potential prey by employing Equation (11).

$$\overrightarrow{D1} = \left|\vec{Y}_{prey_m}(i) - \vec{Y}_{gm}(i)\right| \tag{11}$$

The upgraded location of $the\ mt^h$ grouper is computed by employing Equation (12). It is based on numerous factors, such as the distance $\overrightarrow{D1}$ between the grouper and its prey, k, which defines the outline of a logarithmic spiral, and the predicted prey position at iteration i. Then, the value of $w\ is$ computed by employing Equation (13).

$$\vec{Y}_{gm}(h+1) = \overrightarrow{D1}.e^{kw}cos(2\pi w) + \vec{Y}(_{prey_m}i) \tag{12}$$

$$w = 1 - \frac{2*h}{P_{encircle}} \tag{13}$$

The moray eel's locations are upgraded in this stage by employing Equations (14)-(17).

$$\vec{\lambda}(i) = \left|\vec{Y}_{Em}(i) - \vec{Y}_{prey_m}(i)\right| \tag{14}$$

$$\vec{\eta}(i) = \vec{\lambda}(i) * \xi \tag{15}$$

$$= \frac{The\ distance\ between\ the\ hops}{Total\ no.of\ hops} 2\pi \tag{16}$$

$$Y_E^{i+1} = \alpha * \vec{\lambda}(i) * \xi^* sin(g) + Y_E^i \tag{17}$$

Here, $\vec{\lambda}(i)$ means the difference between the locations of the moray eel and its prey, and the wave amplitude ($\vec{\eta}(i)$) is defined by multiplying $\vec{\lambda}(i)$ by the factor ξ. ξ owns a stochastic value in the range of 0 to 1. α refers to a randomly generated value, and $\sin(g)$ means a value of the sine angle. In the AC phase, every search agent is involved in an attack on the prey after precisely enclosing its position by building a loop with the prey located at its midpoint. The process for finding the circle around the expected prey is as follows: firstly, the position of an agent displaying an optimal fitness function is recognized as the position of the expected prey. Then, the distance between the predicted prey and the other agents is computed. Next, a circle is recognized around the prey, with a radius (R) that signifies the distance from the prey

to the distant agent. To assist many search agents and minimize computational complexity, the radius of the following circle is defined using Equation (18).

$$R_{i+1} = (1 - \mu) * R_i \tag{18}$$

Here, μ represents a shrinking ratio. In the BGME model, the Fitness Function (FF) balances minimizing the number of selected features and maximizing classifier accuracy using those features. Equation (19) indicates the FF used for assessing the solution.

$$Fitness = \alpha\gamma_R(D) + \beta\frac{|R|}{|C|} \tag{19}$$

While $\gamma_R(D)$ means the classifier rate of error of a presumed classifier. $|R|$ refers to the cardinality of the chosen subset. $|C|$ denotes the entire number of features in the dataset, α and β indicate the two parameters that correspond to the significance of classifier merit and sub-set span. $\in$ [1,0] and $\beta = 1 - \alpha$.

3.3. Stage III: Patient Health Care Monitoring using SNN

For the classification process, the EHCMS-MOASNN technique designs an SNN model. The SNN structure is an NN method, which processes data over the time of action potentials or individual spikes [29]. The ability of the SNN to delay the activation of all neurons, by comparison with CNNs, increases the quality score of all neurons. The threshold values of the neighboring neuron are changed once the neuron is activated, which affects whether or not these neurons will fire in response to the upcoming input. If the neuron exceeds the threshold value, neighboring neurons may be activated, generating the flow of activation. In Spiking Neural Networks (SNN), the firing of a neuron relies on its threshold value being surpassed by arriving pulses or spikes. An activity of the neuron may become cooperative if it does not receive sufficient input to reach its threshold value within the provided period of time. SNNs are computationally related to conventional ANNs, always generally. As SNN cannot directly perform analogue computations, one must initially convert the analogue value to the spike's amount of time entering it into SNN, which then outputs the preferred outcomes in the spike category.

$$t = \frac{T_{max}}{1 + e^{(\sigma(128-p)}} \tag{20}$$

Whereas p refers to the overall data in the interval, t signifies the period of time the spike fired, denotes the code's nonlinear value, and $T_{\max}$ signifies the maximal fringe time, fixed at 50 ms. The spike signals $s_i(t)$ are displayed as 0 or 1 in ms time steps, utilizing the rules of STDP. In additional details, a spike is exemplified by the 1ms pulse of unit amplitude; then, there is no spike in relation to 0. Implementing a memory potential, $V(t)$, that is, signified as the rules of STDP in every kth input neuron.

$$V(t) = \sum_{k=1}^{N} w_k\, s_k(t) \tag{21}$$

After $w_k s_k(t)$ generates a postsynaptic potential, and w_k refers to the equivalent weight (synapse) of the input neuron. When the potential membrane $V(t)$ at time t surpasses a given threshold.

$$V(t) > \varphi \tag{22}$$

After the output neuron fires. The weighted dynamics are calculated utilizing the synaptic trace to accelerate model performance. A random BackPropagation (BP) approach is applied for training the unsupervised SNN. The cost function of the LSP is described as

$$L_{sp} = 0.5 \sum_i \left(v_i^p(t) - v_i^l(t)\right)^2 \tag{23}$$

The weights (w_{ij}) updated model in the network is as demonstrated:

$$\frac{\partial L_{sp}}{\partial w_{ij}} = -\sum_i e_i\,(t)\frac{\partial v_i^p(t)}{\partial w_{ij}} \tag{24}$$

Here, $v^l$and v^prepresents the activation rates of the labelled and prediction neurons, correspondingly, and $e_i(t)$ signifies the error of the ith output neuron. Equation (25) is further separated into Equation (25). Figure 3 depicts the infrastructure of SNN.

$$\Delta w_{ij}^c \propto \begin{cases} -\sum_k g_{ik}\, e_k^E, if\ s_j^c(t) and\ b_{min} < I_j(t) < b_{max} \\ 0, Otherwise \end{cases} \tag{25}$$

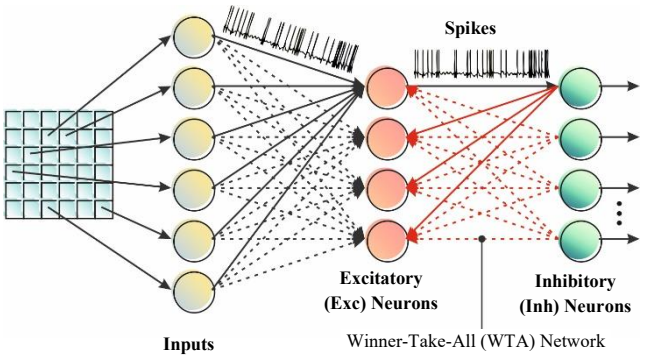

Fig. 3 Structure of the SNN model

Now, $e_k^{E^1}$ signifies the error term neuron in the kth output neuron layer, $I(t)$ denotes the present flow into the ith neuron, $s_j^c(t)$ designates the existence of a presynaptic spike, $b_{\max}$ and $b_{\min}$ represent the current maximum and minimum limits, and g_{ik} means fixed randomly generated numbers.

3.4. Stage IV: Parameter Fine-Tuning using MGO

Additionally, the MGO-based hyperparameter tuning is performed to optimize the classification outcomes of the SNN model. The MGO is a modern population-based searching model that depends on the migration patterns of gazelles searching for food [30]. This search model encompasses four major regions of a gazelle's life: solitary individuals, bachelor male herds, territorial males, maternity herds, and migration for food. During the process of searching, every gazelle goes with a bachelor male herd, a maternity herd, a territorial male group, or is solitary. Each one of the groups can yield a novel gazelle. A mature male gazelle in a group territory exemplifies the optimal global solution for the MGO approach.

3.4.1. Territorial Solitary Males

Male mountain gazelles establish territories after reaching adulthood and sufficient strength. They are highly territorial, maintaining large distances between territories. Adult males fight for territory and female custody, with older males defending their areas while younger males attempt to take over territories and females. The mature male territory is forecasted using Equation (26).

$$TSM = male_{gazelle} - (ri_1 \times BH - ri_2 \times X(t) \times F) \times Cof_r \quad (26)$$

The position vector of adult males, signifying the finest global solution, is given by Equation (26). The variables ri_2 and ri_1 are random integers, both 1 and 2. The vector of coefficients for the younger male herd is considered to be BH, and it is expressed employing Equation (27), which is also used to compute F. The vector of coefficients Cof_r is randomly generated and automatically upgraded in every iteration to enhance the searching ability signified by Eq. (27).

$$BH = X_{ra} \times [r_1] + M_{pr} \times [r_2], ra = \left\{\left[\frac{N}{3}\right] \ldots .\right\} \quad (27)$$

In Equation (25), the randomly generated solution X_{ra} falls in the ra range. The average count of the arbitrarily selected searching agents, $N/3$, is denoted as Mpr. N specifies the overall gazelles, whereas r_2 and r_1 are arbitrary numbers among the values of 1 and 0.

$$F = N_1 \times (D) \times exp\left(2 - Iter \times \left(\frac{2}{MaxIter}\right)\right) \quad (28)$$

$Iter$ specified the existing iteration counts, N_1 represents a randomly chosen integer from the standard distribution of problem dimensions. $MaxIter$ indicates the total iteration counts, and exp specifies an expression for the Exponential function.

$$Cof_i = \begin{cases} (a+1) + r_3 \\ a \times N_2(D) \\ r_4(D) \\ N_3(D) \times N_4(D)^2 \times cos\big((r_4 \times 2) \times N_3(D)\big) \end{cases} \quad (29)$$

Equation (29) is utilized to compute $'a$ in Equation (30). The r_4, r_3, and $rand$ values specify random integers among 0 and 1. N_3, N_4, and $N_{2,}$ are arbitrary numbers that fall within the normal range and size of the problem. Likewise, in terms of the problem size, r_4 represents an arbitrary integer in the range of 0 to 1. Finally, cos is the function of Cosine.

$$a = -1 + Iter \times \left(\frac{-1}{MaxIter}\right) \quad (30)$$

At last, in Eq. (30), $Iter$ is the existing iteration, and $MaxIter$ denotes the existing iteration count.

3.4.2. Maternity Herds

Mountain gazelles considerably depend on maternity herds to guarantee the birth of healthy male offspring that perform crucial roles in their lifecycle. Moreover, aiding females and younger male gazelles in hunting to ensure that they can assist in the birthing process.

$$MH = \big(BH \times Cof_{1,r}\big) + \big(ri_3 \times male_{gazelle} - ri_4 \times X_{rand}\big) \times Cof_{1,r} \quad (31)$$

Equation (31) is utilized to express the influence factor vector of younger males, specifying a BH in Equation (32). In Eq. (29), the coefficients $Cof_{3,r}$ and $Cof_{2,r}$ are arbitrarily chosen vectors. The integers 1 or 2 are employed to establish the values of ri_4 and ri_3. The adult male gazelle currently serves as the optimal global solution. At last, X_{rand} relates to the location vector of an arbitrarily chosen gazelle in relation to the overall population.

3.4.3. Bachelor Male Herds

As male gazelles' strategy matures, they determine territory and assert control over female groups. In this stage, younger male gazelles challenge older males in aggressive battles for power and dominance through the females, frequently leading to violent confrontations.

$$BMH = (X(t) \times D) + \big(ri_5 \times male_{gazelle} - ri_6 \times BH\big) \times Cof_r \quad (32)$$

The location of the gazelle vector in the existing iteration is depicted as $X(t)$ in Equation (33). Simultaneously, Equation (33) is employed to compute D. Random integers ri_6 and ri_5 are chosen, both 1 and 2 correspondingly. The optimum solution matches the position of the vector of the male gazelle, signifying the prevailing male gazelle. Furthermore, BH specifies the effective aspect of the younger male herd, as defined by Equation (32), whereas Cof_r is calculated using Equation (33).

$$D = \big(|X(t)| + \big|male_{gazelle}\big|\big) \times (2 \times r_6 - 1) \quad (33)$$

Equation (33) establishes the location of gazelle vectors in the existing iteration, denoted as $X(t)$ and the male gazelle, correspondingly. The position vector denotes the optimum solution, with r 6 being another arbitrary number created between 0 and 1.

3.4.4. Migration to Search for Food

Mountain gazelles travel longer distances to hunt food, continually hunting novel food resources. They are represented by their swift running gait and exceptional jumping capability. The mathematical expression of this behaviour of the gazelle is given.

$$MSF = (ub - lb) \times r_7 + lb \quad (34)$$

The lower and upper bounds of issues are depicted in Eq. (33) as lb and ub, respectively. Likewise, r_7 denotes an arbitrarily created integer between 0 and 1. Finally, in every iteration, the gazelles are graded in ascending order depending on their performance. The top-performing gazelles provide promising and superior solutions, whereas older or weaker individuals are taken away from the population. The foremost adult male gazelle holding the territory is considered the optimum solution. The MGO model develops an FF to achieve enhanced classification performance. It defines an optimistic number to signify the better efficiency of the candidate solution. The classifier error rate reduction is measured as FF, as detailed in Equation (35).

$$fitness(x_i) = ClassifierErrorRate(x_i)$$

$$= \frac{No.of\ misclassified\ samples}{Total\ no.of\ samples} \times 100 \quad (35)$$

4. Experimental Result and Analysis

The performance evaluation of the EHCMS-MOASNN technique is tested using the Healthcare IoT dataset from the Kaggle repository [31]. The dataset includes 200 samples with two classes, as shown in Table 1. This dataset simulates sensor data collected from wearable devices in an IoT-based healthcare system.

The data corresponds to patient health monitoring with sensors that measure various vital signs. These sensors, such as temperature, blood pressure, heart rate, and battery level, provide real-time information that is transmitted to healthcare providers for remote monitoring. It contains a total of 13 features, out of which 11 are selected.

Table 1. Details of the dataset

Health Status	No. of Instances
Unhealthy (in need of medical attention)	113
Healthy	87
Total Instances	200

Figure 4 reports a set of confusion matrices generated by the EHCMS-MOASNN model on 500-3000 epochs. After 500 epochs, the EHCMS-MOASNN model has recognized 110 samples as unhealthy and 77 samples as healthy. Following this, at 1000 epochs, the EHCMS-MOASNN technique identified 110 samples as unhealthy and 78 samples as healthy. Likewise, on 2000 epochs, the EHCMS-MOASNN approach recognized 110 samples as unhealthy and 85 samples as healthy. Finally, after 3000 epochs, the EHCMS-MOASNN model recognized 111 samples as unhealthy and 87 samples as healthy.

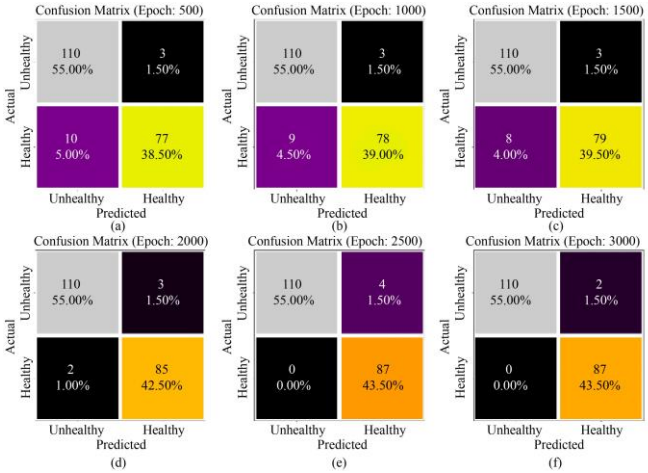

Fig. 4 Confusion matrices of EHCMS-MOASNN model (a-f) 500-3000 epochs

In Table 2 and Figure 5, the classification results of the EHCMS-MOASNN technique are clearly depicted under 500-3000 epochs. The results indicated that the EHCMS-MOASNN technique effectively distinguished between unhealthy and healthy samples. With 500 epochs, the EHCMS-MOASNN technique gains an average $accu_y$ of 92.93%, $prec_n$ of 93.96%, $sens_y$ of 92.93%, $spec_y$ of 92.93%, $F1_{score}$ of 93.32%, and MCC of 86.88%. Also, based on 1000 epochs, the EHCMS-MOASNN approach attains an average $accu_y$ of 93.50%, $prec_n$ of 94.37%, $sens_y$ of 93.50%, $spec_y$ of 93.50%, $F1_{score}$ of 93.84%, and MCC of 87.86%. Concurrently, using 2000 epochs, the EHCMS-MOASNN approach receives an average $accu_y$ of 97.52%, $prec_n$ of 97.40%, $sens_y$ of 97.52%, $spec_y$ of 97.52%, $F1_{score}$ of 97.46%, and MCC of 94.93%. Simultaneously, based on 2500 epochs, the EHCMS-MOASNN approach obtains an average $accu_y$ of 98.23%, $prec_n$ of 97.80%, $sens_y$ of 98.23%, $spec_y$ of 98.23%, $F1_{score}$ of 97.98%, and MCC of 96.03%. At last, on 3000 epochs, the EHCMS-MOASNN approach accomplishes an average $accu_y$ of 99.12%, $prec_n$ of 98.88%, $sens_y$ of 99.12%, $spec_y$ of 99.12%, $F1_{score}$ of 98.99%, and MCC of 97.99%.

In Figure 6, the TRAAY and VLAAY $accu_y$ of the EHCMS-MOASNN technique is illustrated on 500-3000

epochs. In addition, the TRAAY and VLAAY methods mitigate overfitting throughout the epochs, resulting in improved performance of the EHCMS-MOASNN approach and ensuring steady calculations on unseen samples. The result indicates the proficiency of the EHCMS-MOASNN technique, with optimal performance across multiple repetitions.

Table 2. Classifier outcome of EHCMS-MOASNN model under 500-3000 epochs

Classes	$Accu_y$	$Prec_n$	$Sens_y$	$Spec_y$	$F1_{Score}$	MCC
Epoch - 500						
Unhealthy	97.35	91.67	97.35	88.51	94.42	86.88
Healthy	88.51	96.25	88.51	97.35	92.22	86.88
Average	**92.93**	**93.96**	**92.93**	**92.93**	**93.32**	**86.88**
Epoch - 1000						
Unhealthy	97.35	92.44	97.35	89.66	94.83	87.86
Healthy	89.66	96.30	89.66	97.35	92.86	87.86
Average	**93.50**	**94.37**	**93.50**	**93.50**	**93.84**	**87.86**
Epoch – 1500						
Unhealthy	97.35	93.22	97.35	90.80	95.24	88.85
Healthy	90.80	96.34	90.80	97.35	93.49	88.85
Average	**94.07**	**94.78**	**94.07**	**94.07**	**94.36**	**88.85**
Epoch - 2000						
Unhealthy	97.35	98.21	97.35	97.70	97.78	94.93
Healthy	97.70	96.59	97.70	97.35	97.14	94.93
Average	**97.52**	**97.40**	**97.52**	**97.52**	**97.46**	**94.93**
Epoch - 2500						
Unhealthy	96.46	100.00	96.46	100.00	98.20	96.03
Healthy	100.00	95.60	100.00	96.46	97.75	96.03
Average	**98.23**	**97.80**	**98.23**	**98.23**	**97.98**	**96.03**
Epoch - 3000						
Unhealthy	98.23	100.00	98.23	100.00	99.11	97.99
Healthy	100.00	97.75	100.00	98.23	98.86	97.99
Average	**99.12**	**98.88**	**99.12**	**99.12**	**98.99**	**97.99**

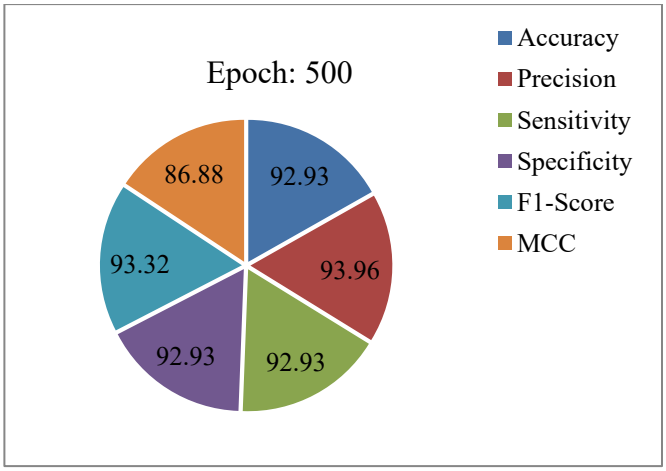

(a)

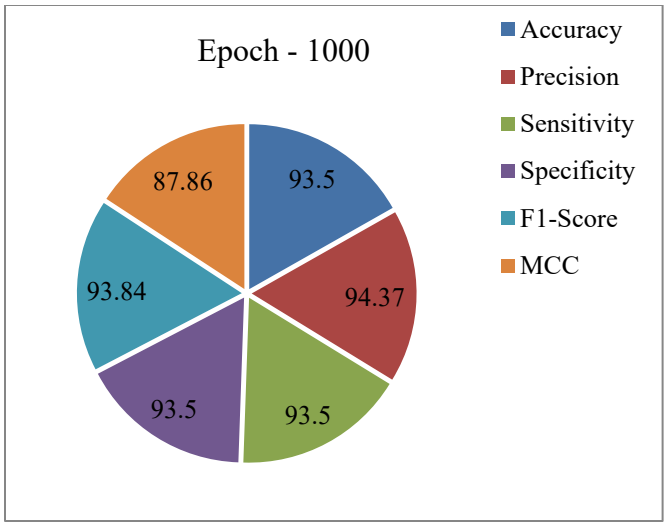

(b)

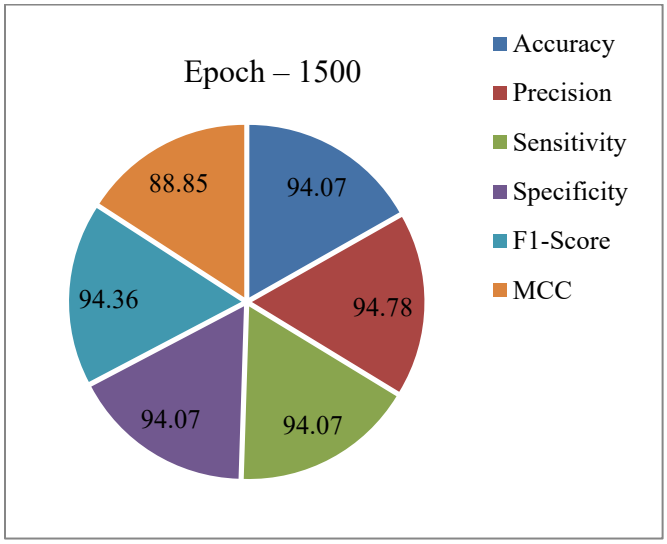

(c)

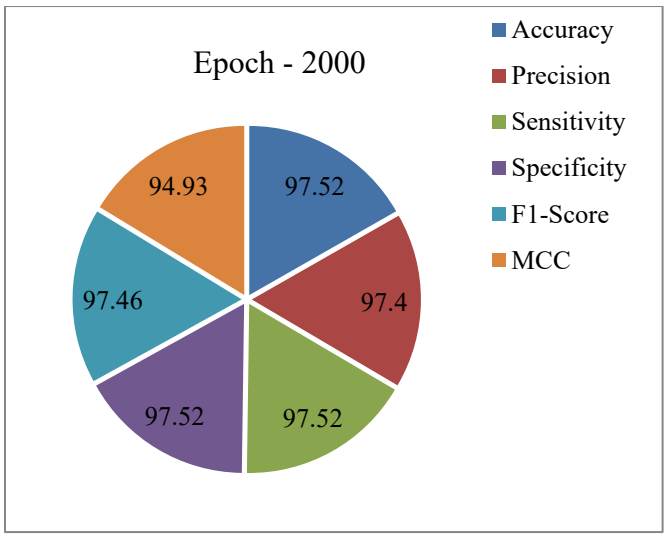

(d)

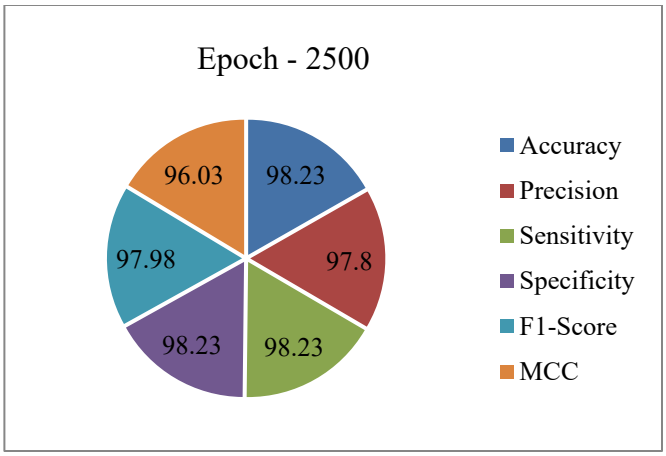

(e)

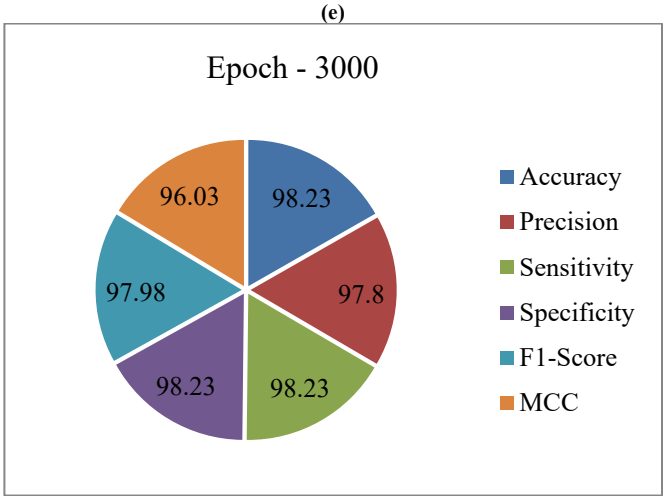

(f)

Fig. 5 Average of EHCMS-MOASNN model (a-f) 500-3000 epochs

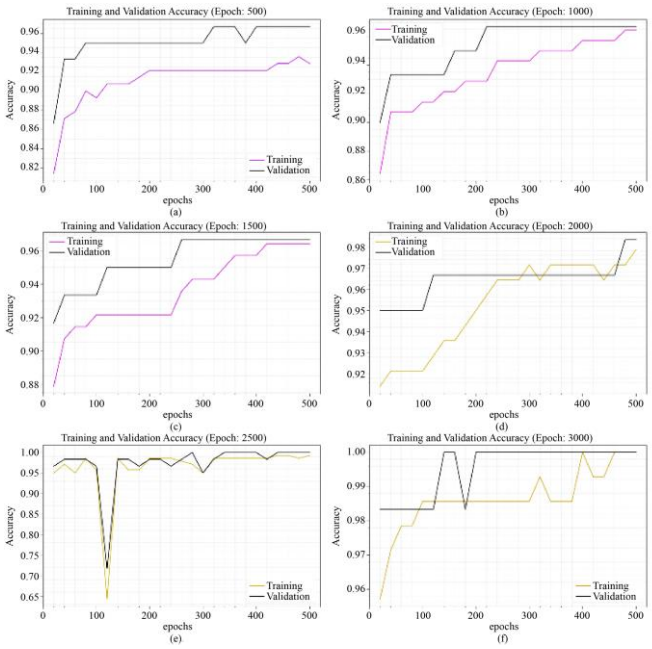

Fig. 6 $Accu_y$ curve of EHCMS-MOASNN model (a-f) 500-3000 epochs

In Figure 7, the TRA loss (TRALO) and VLA loss (VLALO) graphs of the EHCMS-MOASNN approach based on 500-3000 epochs are showcased. It is exemplified that the TRALO and VLALO values demonstrate a lessening propensity. The successive dilution in loss values, as well as the use of securities, enhances the higher outcome of the EHCMS-MOASNN method and gradually tunes the calculation outputs.

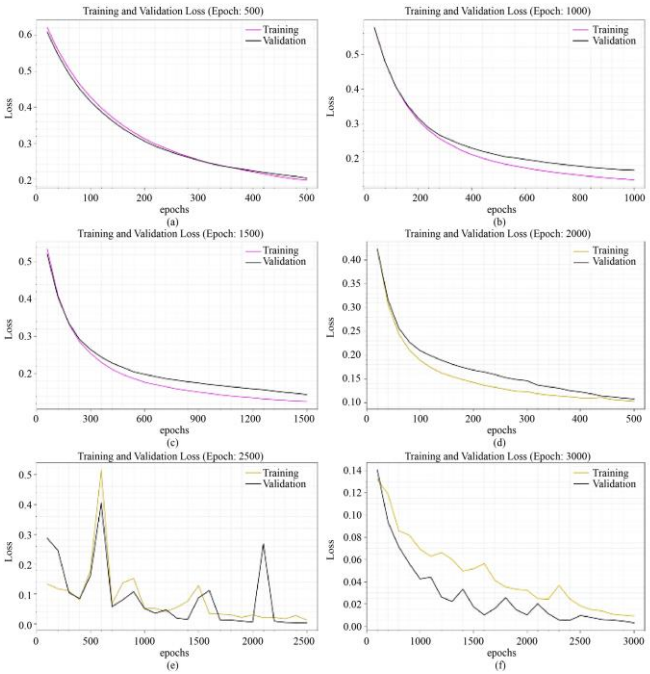

Fig. 7 Loss curve of EHCMS-MOASNN model (a-f) 500-3000 epochs

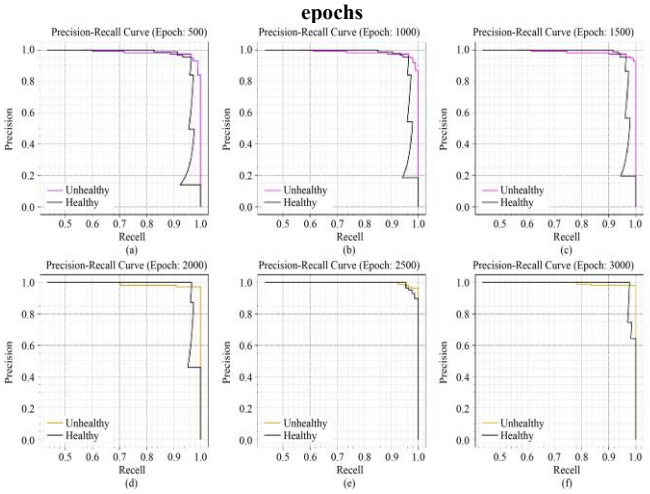

Fig. 8 PR curve of EHCMS-MOASNN model (a-f) 500-3000 epochs

In Figure 8, the Precision-Recall (PR) curve outcome of the EHCMS-MOASNN technique, evaluated across 500 to 3000 epochs, assesses its classification performance by plotting PR for all classes. The constant increase in PR values across all classes indicates the model's efficacy in accurately distinguishing class instances.

In Figure 9, the Receiver Operating Characteristic (ROC) curve of the EHCMS-MOASNN approach is analyzed through 500 to 3000 epochs. The performances represent an enhancement in ROC values over all classes, illustrating the model's strong discriminative capability. The consistent trend of improved ROC outcomes through multiple classes further confirms the EHCMS-MOASNN model's robustness and reliability in the classification process.

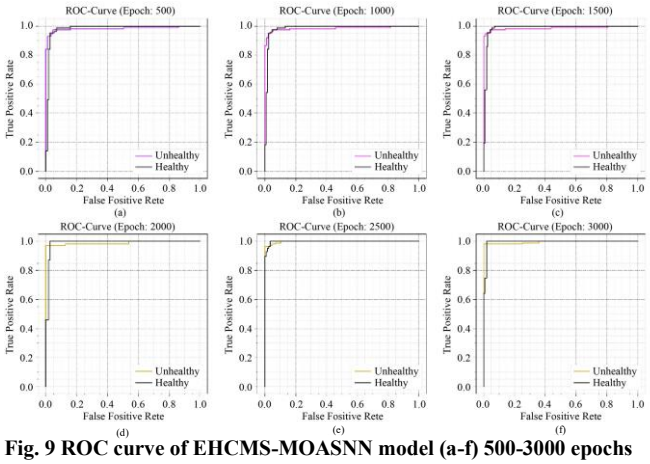

Fig. 9 ROC curve of EHCMS-MOASNN model (a-f) 500-3000 epochs

To illustrate the capabilities of the EHCMS-MOASNN model, a detailed comparison of the outcomes is presented in Table 3 [32-34].

In Figure 10, a comparative $accu_y$, $prec_n$, and $F1_{score}$ outcomes of the EHCMS-MOASNN method are delivered. The performances imply that the CNN-BiLSTM-GRU, AI-IoT, and HMS-ITM methodologies have yielded poorer values of $accu_y$, $prec_n$, and $F1_{score}$. Simultaneously, the DNN and KNN methodologies have shown a marginally increased $accu_y$, $prec_n$, and $F1_{score}$. In the meantime, the SIoT-SHMS and Deep ConvNet methodologies have yielded more accurate values of $accu_y$, $prec_n$, and $F1_{score}$. However, the EHCMS-MOASNN method provides enhanced performance with $accu_y$, $prec_n$, and $F1_{score}$of 99.12%, 98.88%, and 98.99%, respectively.

In Figure11, comparative $sens_y$ and $spec_y$ outcomes of the EHCMS-MOASNN model are presented. The performances suggest that the HMS-ITM, CNN-BiLSTM-GRU, and DNN approaches have provided poorer values of $sens_y$ and $spec_y$. Similarly, the AI-IoT and KNN approaches have achieved marginally higher $sens_y$ and $spec_y$. Likewise, the SIoT-SHMS and Deep ConvNet approaches have provided closer values of $sens_y$ and $spec_y$. However, the EHCMS-MOASNN method achieved its maximum outcome with $sens_y$ and $spec_y$ of 99.12% and 99.12%, respectively.

Table 3. Comparative outcome of the EHCMS-MOASNN method with other existing models

Technique	$Accu_y$	$Prec_n$	$Sens_y$	$Spec_y$	$F1_{Score}$
Deep ConvNet	98.77	89.02	94.84	98.49	89.29
AI-IoT	91.86	98.28	92.76	90.87	97.42
SIoT-SHMS	96.83	95.61	93.20	94.64	93.62
HMS-ITM	92.05	96.01	89.02	93.96	89.87
KNN Algorithm	94.25	92.17	92.89	89.39	94.68
CNN-BiLSTM-GRU	90.13	93.88	90.16	92.28	92.66
DNN Algorithm	92.33	89.78	90.44	91.49	94.27
EHCMS-MOASNN	99.12	98.88	99.12	99.12	98.99

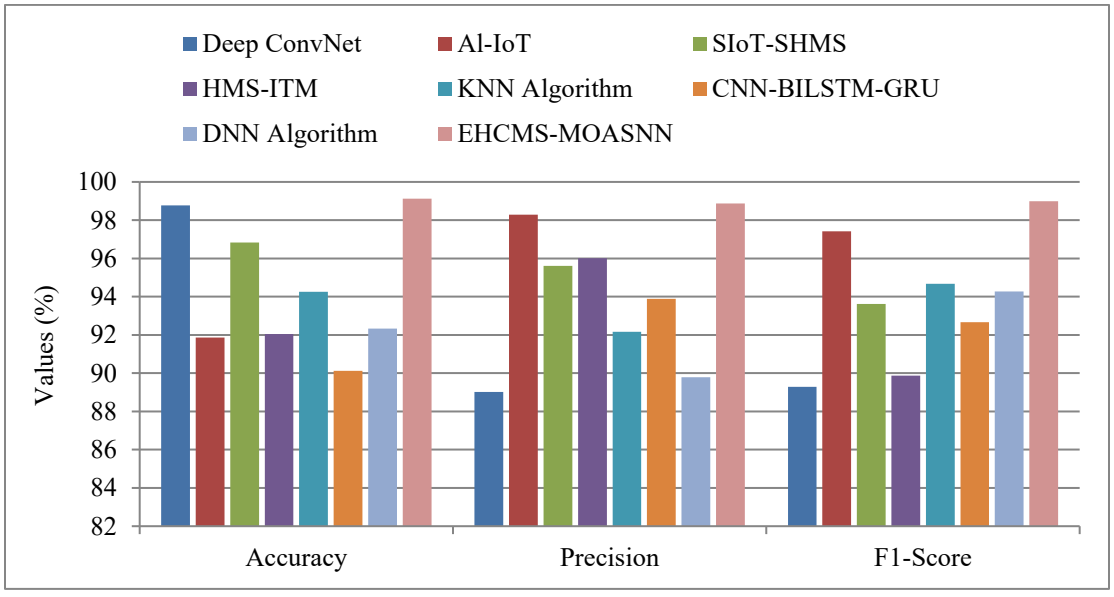

Fig. 10 ccu_y, $prec_n$, and $F1_{score}$ of the EHCMS-MOASNN technique with other models

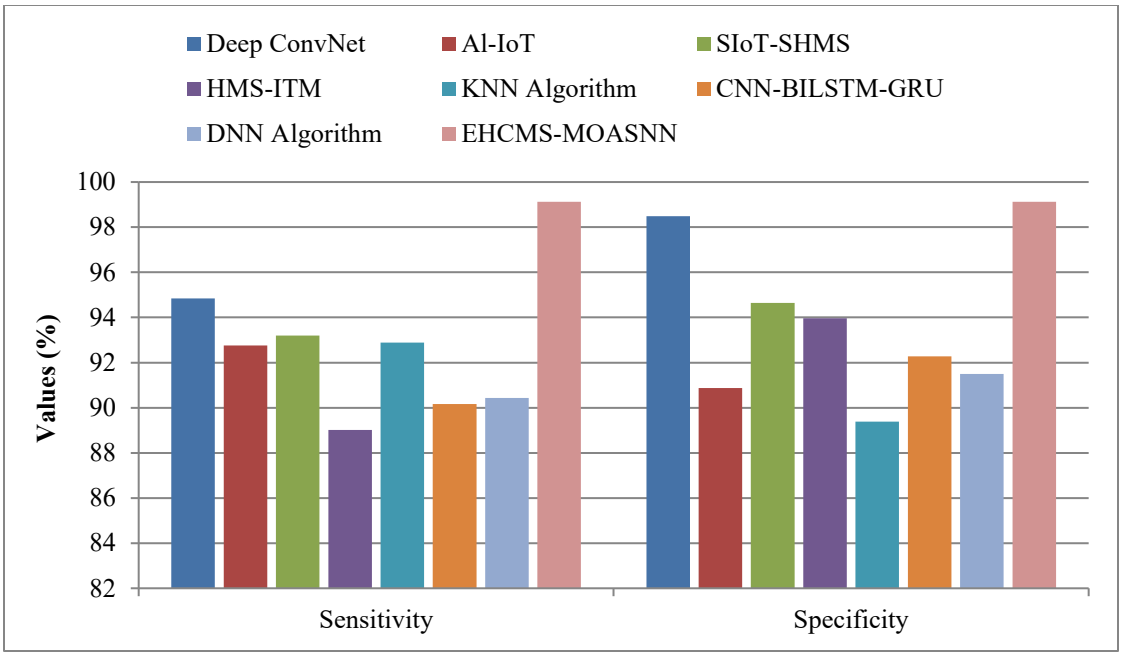

Fig. 11 $Sens_y$ and $spec_y$ of the EHCMS-MOASNN technique with other models

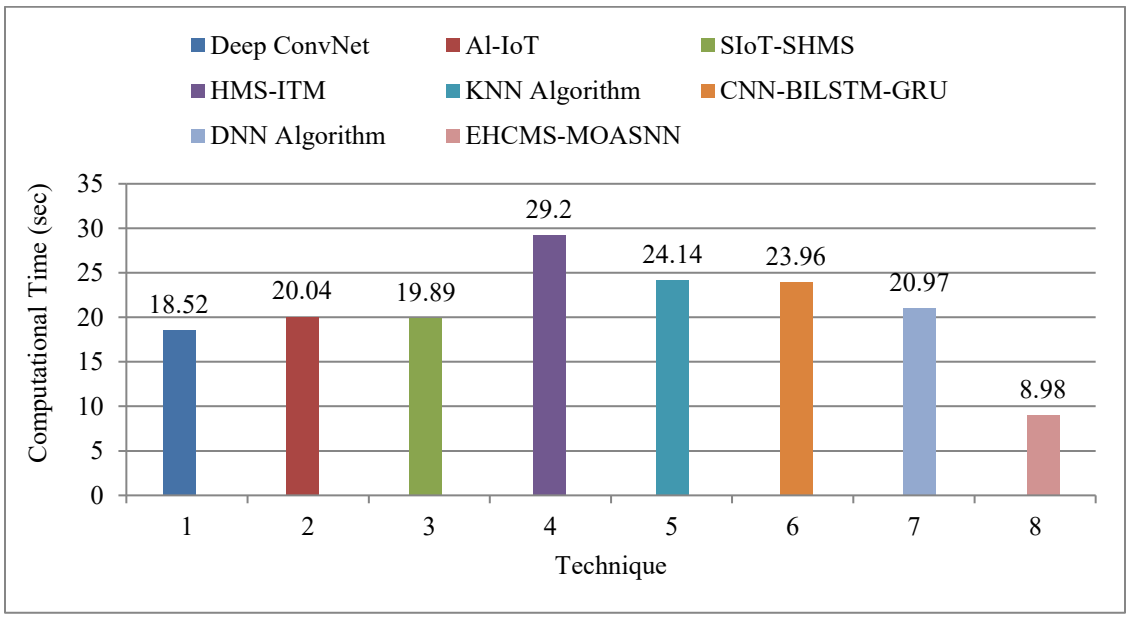

Fig. 12 COMT outcome of the EHCMS-MOASNN approach with other models

The Computation Time (COMT) outcomes of the EHCMS-MOASNN method are compared with other methodologies in Table 4 and Figure 12. The performance shows that the EHCMS-MOASNN approach achieves a lower COMT of 8.98s.

Alternatively, the Deep ConvNet, AI-IoT, SIoT-SHMS, HMS-ITM, KNN, CNN-BiLSTM-GRU, and DNN techniques gain improved COMT values of 18.52s, 20.04s, 19.89s, 29.20s, 24.14s, 23.96s, and 20.97s, respectively.

Table 4. COMT outcome of the EHCMS-MOASNN approach with other models

Technique	Computational Time (sec)
Deep ConvNet	18.52
AI-IoT	20.04
SIoT-SHMS	19.89
HMS-ITM	29.20
KNN Algorithm	24.14
CNN-BiLSTM-GRU	23.96
DNN Algorithm	20.97
EHCMS-MOASNN	8.98

5. Conclusion

In this paper, we have presented an EHCMS-MOASNN model for smart diagnosis in IoT. The model aimed to develop an advanced healthcare monitoring system for the medical sector, utilizing advanced models. Initially, the min-max scaling method was used for pre-processing. Additionally, the FS process was implemented using the BGME optimization algorithm to detect and select the most relevant and significant features in the input data. For the classification process, the SNN model was employed. Additionally, the MGO-based hyperparameter range procedure was performed to optimize the classification outcomes of the SNN model. The EHCMS-MOASNN method's efficiency is validated on the Healthcare IoT dataset, achieving a superior accuracy of 99.12% compared to recent techniques.

Data Availability Statement

The data that support the findings of this study are openly available in the Kaggle repository at https://www.kaggle.com/datasets/ziya07/healthcare-iot-data, reference number [31].

References

[1] Shreshth Tuli et al., "HealthFog: An Ensemble Deep Learning-Based Smart Healthcare System for Automatic Diagnosis of Heart Diseases in Integrated IoT and Fog Computing Environments," *Future Generation Computer Systems*, vol. 104, pp. 187-200, 2020. [CrossRef] [Google Scholar] [Publisher Link]

[2] Farman Ali et al., "A Smart Healthcare Monitoring System for Heart Disease Prediction Based on Ensemble Deep Learning and Feature Fusion," *Information Fusion*, vol. 63, pp. 208-222, 2020. [CrossRef] [Google Scholar] [Publisher Link]

[3] Wei Li et al., "A Comprehensive Survey on Machine Learning-Based Big Data Analytics for IoT-Enabled Smart Healthcare System," *Mobile Networks and Applications*, vol. 26, pp. 234-252, 2021. [CrossRef] [Google Scholar] [Publisher Link]

[4] Pavleen Kaur, Ravinder Kumar, and Munish Kumar, "A Healthcare Monitoring System using Random Forests and Internet of Things (IoT)," *Multimedia Tools and Applications*, vol. 78, pp. 19905-19916, 2019. [CrossRef] [Google Scholar] [Publisher Link]

[5] Joseph Futoma et al., "The Myth of Generalisability in Clinical Research and Machine Learning in Health Care," *The Lancet Digital Health*, vol. 2, no. 9, pp. e489-e492, 2020. [Google Scholar] [Publisher Link]

[6] Xiaokang Zhou et al., "Deep-Learning-Enhanced Human Activity Recognition for Internet of Healthcare Things," *IEEE Internet of Things Journal*, vol. 7, no. 7, pp. 6429-6438, 2020. [CrossRef] [Google Scholar] [Publisher Link]

[7] Mazin Alshamrani, "IoT and Artificial Intelligence Implementations for Remote Healthcare Monitoring Systems: A Survey," *Journal of King Saud University - Computer and Information Sciences*, vol. 34, no. 8, pp. 4687-4701, 2022. [CrossRef] [Google Scholar] [Publisher Link]

[8] Taher M. Ghazal et al., "IoT for Smart Cities: Machine Learning Approaches in Smart Healthcare—A Review," *Future Internet*, vol. 13, no. 8, pp. 1-19, 2021. [CrossRef] [Google Scholar] [Publisher Link]

[9] Safa Ben Atitallah et al., "Leveraging Deep Learning and IoT Big Data Analytics to Support the Smart Cities Development: Review and Future Directions," *Computer Science Review*, vol. 38, 2020. [CrossRef] [Google Scholar] [Publisher Link]

[10] R. Venkatesan et al., "Intelligent Smart Dustbin System Using Internet of Things (IoT) for Health Care," *Journal of Cognitive Human-Computer Interaction*, vol. 1, no. 2, pp. 73-80, 2021. [CrossRef] [Google Scholar] [Publisher Link]

[11] R. Vasanth, M. Paranthaman, and P. Sivaprakash, *ML and IoT Coupled Biomedical Applications in Healthcare: Smart Growth and Upcoming Challenges*, 1st ed., Internet of Things Enabled Machine Learning for Biomedical Applications, CRC Press, pp. 1-22, 2024. [Google Scholar] [Publisher Link]

[12] Muthukathan Rajendran Sudha et al., "Predictive Modeling for Healthcare Worker Well-Being with Cloud Computing and Machine Learning for Stress Management," *International Journal of Electrical & Computer Engineering*, vol. 15, no. 1, pp. 1218-1228, 2025. [CrossRef] [Google Scholar] [Publisher Link]

[13] J. Malathi et al., "IoT-Enabled Remote Patient Monitoring for Chronic Disease Management and Cost Savings: Transforming Healthcare," *Advances in Explainable AI Applications for Smart Cities*, IGI Global, pp. 371-388, 2024. [Google Scholar]

[14] Ali Hamza Najim et al., "An IoT Healthcare System with Deep Learning Functionality for Patient Monitoring," *International Journal of Communication Systems*, vol. 38, no. 4, 2025. [CrossRef] [Google Scholar] [Publisher Link]

[15] S. Rajarajan et al., "IoT-Enabled Respiratory Pattern Monitoring in Critical Care: A Real-Time Recurrent Neural Network Approach," *10th International Conference on Communication and Signal Processing*, Melmaruvathur, India, pp. 508-513, 2024. [CrossRef] [Google Scholar] [Publisher Link]

[16] Prabhat Kumar et al., "A Blockchain-Orchestrated Deep Learning Approach for Secure Data Transmission in IoT-Enabled Healthcare System," *Journal of Parallel and Distributed Computing*, vol. 172, pp. 69-83, 2023. [CrossRef] [Google Scholar] [Publisher Link]

[17] B.D. Parameshachari et al., "Healthcare Monitoring of Patient Using CNN Based Model in Internet of Things," *International Conference on Applied Intelligence and Sustainable Computing*, Dharwad, India, pp. 1-6, 2023. [CrossRef] [Google Scholar] [Publisher Link]

[18] Ashish Khanna et al., "Internet of Things and Deep Learning Enabled Healthcare Disease Diagnosis using Biomedical Electrocardiogram Signals," *Expert Systems*, vol. 40, no. 4, 2023. [CrossRef] [Google Scholar] [Publisher Link]

[19] Vobbilineni Thrimurthulu et al., "Advanced Automatic Healthcare Monitoring System for IoT-Based Context-Aware Architecture Using Optimized Periodic Implicit Generative Adversarial Networks," *Smart Science*, pp. 1-13, 2025. [CrossRef] [Google Scholar] [Publisher Link]

[20] Jagadeesh Basavaiah et al., "An Efficient Approach of Epilepsy Seizure Alert System Using IoT and Machine Learning," *Journal of Reliable Intelligent Environments*, vol. 10, no. 4, pp. 449-461, 2024. [CrossRef] [Google Scholar] [Publisher Link]

[21] P. Mangal, and D. Lakshmi, "Advanced Biomedical Signal Processing Techniques for Real-Time Health Monitoring Systems," *Deep Learning in Medical Signal and Image Processing*, pp. 45-62, 2025. [Google Scholar]

[22] R. Arivalahan, and T. Vinoth, "Health Monitoring in IoT with Context-Aware Deep Convolutional Spiking Neural Network and Woodpecker Mating Algorithm," *IETE Journal of Research*, vol. 70, no. 7, pp. 6494-6504, 2024. [CrossRef] [Google Scholar] [Publisher Link]

[23] Akash Ghosh et al., "Blockchain-Assisted Serverless Framework for AI-Driven Healthcare Applications," *International Journal of Advanced Computer Science & Applications*, vol. 16, no. 5, pp. 473-482, 2025. [CrossRef] [Google Scholar] [Publisher Link]

[24] P.B. Suryawanshi et al., "An Efficient IoT-based Patient Monitoring System for Heart Disease Prediction and Categorization using Optimized Cell Attention based Spiking Neural Network," *8th International Conference on I-SMAC (IoT in Social, Mobile, Analytics and Cloud)(I-SMAC)*, pp. 47-54, 2024. [CrossRef] [Google Scholar] [Publisher Link]

[25] Asma Alshuhail et al., "Machine Edge-Aware IoT Framework for Real-Time Health Monitoring: Sensor Fusion and AI-Driven Emergency Response in Decentralized Networks," *Alexandria Engineering Journal*, vol. 129, pp. 1349-1361, 2025. [CrossRef] [Google Scholar] [Publisher Link]

[26] Abhiraj Gautam, and Sachin Sharma, "Artificial Narrow Intelligence Inspired Neuromorphic Computing for Logic Operations in Healthcare Appliances," *7th International Conference on Circuit Power and Computing Technologies*, Kollam, India, vol. 1, pp. 714-719, 2024. [CrossRef] [Google Scholar] [Publisher Link]

[27] Poovendran Alagarsundaram et al., "Adaptive CNN-LSTM and Neuro-Fuzzy Integration for Edge AI and IoMT-Enabled Chronic Kidney Disease Prediction," *International Journal of Applied Science Engineering and Management*, vol. 18, no. 3, pp. 553-582, 2024. [Google Scholar] [Publisher Link]

[28] Nehal A. Mansour et al., "Adaptive Disease Diagnosis Strategy (ADDS) Based on Enhanced Incremental Artificial Intelligence," *International Journal of Telecommunications*, vol. 5, no. 1, pp. 1-33, 2025. [CrossRef] [Google Scholar] [Publisher Link]

[29] G.L. Anoop, C. Nandini, and E. Naresh, "3TFL-XLnet-CP: A Novel Transformer-Based Crop Yield Prediction Framework with Weighted Loss Based 3-Tier Feature Learning Model," *SN Computer Science*, vol. 6, no. 3, pp. 1-17, 2025. [CrossRef] [Google Scholar] [Publisher Link]

[30] Efe Francis Orumwense et al., "An Optimal Energy Management Strategy for Microgrids Based on Mountain Gazelle Optimization and Point Estimation Method," *SSRN*, pp. 1-30, 2025. [CrossRef] [Google Scholar] [Publisher Link]

[31] Healthcare IoT Dataset. [Online]. Available: https://www.kaggle.com/datasets/ziya07/healthcare-iot-data

[32] Syed Umar Amin et al., "Cognitive Smart Healthcare for Pathology Detection and Monitoring," *IEEE Access*, vol. 7, pp. 10745-10753, 2019. [CrossRef] [Google Scholar] [Publisher Link]

[33] R.R. Irshad et al., "A Novel Artificial Spider Monkey Based Random Forest Hybrid Framework for Monitoring and Predictive Diagnoses of Patients Healthcare," *IEEE Access*, vol. 11, pp. 77880-77894, 2023. [CrossRef] [Google Scholar] [Publisher Link]

[34] Mirza Akhi, Ciarán Eising, and Lubna Luxmi Dhirani, "TCN-Based DDoS Detection and Mitigation in 5G Healthcare-IoT: A Frequency Monitoring and Dynamic Threshold Approach," *IEEE Access*, vol. 13, pp. 12709-12733, 2025. [CrossRef] [Google Scholar] [Publisher Link]